

Transport of transient solar wind particles in Earth's cusps

G. K. Parks,^{1,a)} E. Lee,¹ A. Teste,¹ M. Wilber,¹ N. Lin,¹ P. Canu,² I. Dandouras,³ H. Rème,³ S. Y. Fu,⁴ and M. L. Goldstein⁵

¹Space Sciences Laboratory, University of California, Berkeley, California 94720, USA

²CETP, Velizy, France

³Centre d'Etude Spatiale des Rayonnements, Paul Sabatier University, Toulouse, France

⁴School of Earth and Space Sciences, Peking University, China

⁵NASA Goddard Space Flight Center, Greenbelt, Maryland 20770, USA

(Received 12 June 2008; accepted 9 July 2008; published online 11 August 2008)

An important problem in space physics still not understood well is how the solar wind enters the Earth's magnetosphere. Evidence is presented that transient solar wind particles produced by solar disturbances can appear in the Earth's mid-altitude ($\sim 5 R_E$ geocentric) cusps with densities nearly equal to those in the magnetosheath. That these are magnetosheath particles is established by showing they have the same "flattop" electron distributions as magnetosheath electrons behind the bow shock. The transient ions are moving parallel to the magnetic field (\mathbf{B}) toward Earth and often coexist with ionospheric particles that are flowing out. The accompanying waves include electromagnetic and broadband electrostatic noise emissions and Bernstein mode waves. Phase-space distributions show a mixture of hot and cold electrons and multiple ion species including field-aligned ionospheric O^+ beams. © 2008 American Institute of Physics.

[DOI: 10.1063/1.2965825]

Earth's magnetic field at high altitudes has funnel-shaped regions called "cusps." The cusp geometry is associated with many magnetic structures, including those of pulsar magnetospheres. Cusp magnetic fields received much attention in early fusion research when ways were sought to trap and confine plasmas. Theoretical analysis has shown that particle trajectories depend on initial phase angles of injected particles and can pass through the "throat" without mirroring^{1,2} or interact with trapped particles exciting instabilities and heat plasma.³

Space plasma observations first recognized the importance of cusps when magnetosheath particles were detected in the polar region.^{4,5} Systematic studies of cusps have been made possible recently by Cluster,⁶ whose apogee and perigee are, respectively, at $\sim 19 R_E$ and $\sim 4 R_E$ and the orbit plane perpendicular to the ecliptic plane. The four spacecraft frequently cut through the mid-altitude ($\sim 5 R_E$) and high-altitude ($>10 R_E$) cusp regions ($R_E \sim 6400$ km). Cluster has shown, for example, that the high-altitude cusps adjacent to the magnetopause are often permeated with large-amplitude waves.⁷ Cluster also has found energetic particles up to several hundred keV in the cusps, corroborating earlier observations.^{8,9} During disturbed solar wind, even energetic >20 keV O^+ ions are detected.¹⁰ Moreover, intense ion fluxes detected at the expected regions of mid-altitude cusps have strengthened the idea that magnetosheath particles are entering the high-altitude cusps.¹¹

We have now quantified the cusp particle observations using transient solar wind density increases produced by solar disturbances. We measure the transient solar wind density first at L_1 and later at high- or mid-altitude cusp regions

depending on whether Cluster is near apogee or perigee. Sixty such transient events have been studied (thirty each at mid- and high-altitudes) covering periods of fast and slow solar wind and northward and southward interplanetary magnetic fields. The same events measured in two different regions have shown that the transient particles at mid-altitude cusps can have densities nearly equal to magnetosheath densities. The electrons accompanying the ions have a "flattop" shape distribution similar to those behind the bow shock,¹² firmly establishing that magnetosheath particles are being detected. Ionospheric particles escape through the same cusp fields that solar wind particles are streaming in. The accompanying waves include whistlers, Debye scale electron holes, and Bernstein mode waves.

Previous observations have shown that "pressure pulses" associated with transient solar wind density increases can intensify the dynamic aurora,¹³ trigger a substorm,¹⁴ and excite traveling convection vortices.¹⁵ However, there have been no reports about the pressure pulse particles entering the cusps.

The solar wind transients are easy to recognize by their higher densities and lower temperature than the unperturbed solar wind.¹⁶ Below are shown two transient events that Cluster intercepted in the magnetosheath (21 June 2007) and mid-altitude cusp (21 October 2001).

A. Solar Wind: Two transient solar wind events observed by ACE are shown in Fig. 1. On 21 June 2007, the quiet (transient) solar wind densities were ~ 5 cc⁻¹ (30 cc⁻¹), bulk speed ~ 370 km s⁻¹ (460 km s⁻¹), temperature $T \sim 10$ eV (3 eV), and $\beta = 2\mu_0 nkT/B^2 \sim 0.2$ (20-80). On 21 October 2001, the quiet (transient) densities were 7 cc⁻¹ (30 cc⁻¹), $V \sim 650$ km s⁻¹ (700 km s⁻¹), $T \sim 20$ eV (5 eV), and $\beta \sim 0.1$ (0.7).

^{a)}Electronic mail: parks@ssl.berkeley.edu

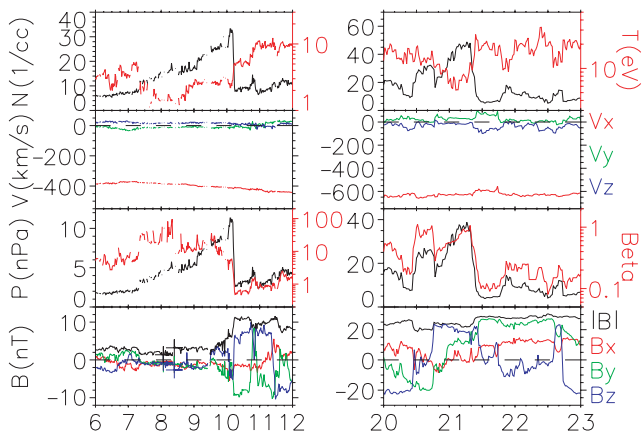


FIG. 1. (Color) Ion bulk parameters (64 s averages) of solar wind (left, 21 June 2007; right, 21 October 2001) for energies ~ 10 eV/q–25 keV/q at L_1 measured by ACE (Advanced Composition Explorer). Shown are n_{sw} , T_{sw} , V_{sw} , β_{sw} , and \mathbf{B} . Solar wind n_{sw} increases are caused by transient solar disturbances.

B. Magnetosheath: The transient retained its shape but the bulk ion parameters changed (Fig. 2). The temperature increased to $T_{msh} \sim 200$ eV and the bulk speeds reduced to $V_x = -300$ km s $^{-1}$ that steadily slowed as Cluster approached the magnetopause ($V_y = -100$ km s $^{-1}$ and $V_z = -30$ km s $^{-1}$). The several magnetopause crossings Cluster encountered, starting ~ 0700 UT, were likely due to dynamic pressure variations in the solar wind. Magnetosphere (magnetosheath) is identified by low ion density \sim a few tenths cc $^{-1}$ (> 10 cc $^{-1}$), high temperature, ~ 2 keV (~ 200 eV), and relatively low (high) bulk speeds < 50 km s $^{-1}$ (~ 200 km s $^{-1}$).

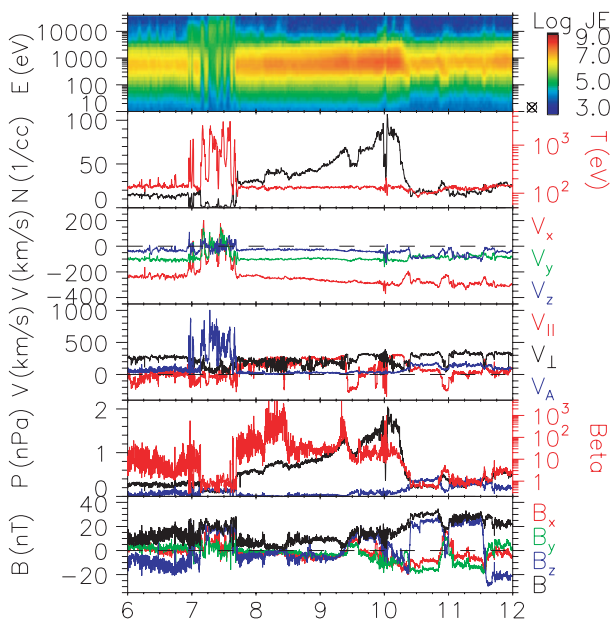


FIG. 2. (Color) Bulk parameters from Cluster 1 (SC1) of the transient in the magnetosheath on 21 June 2007 (~ 15 eV to 35 keV/charge). From top to bottom are spin averaged data (4s) of the energy spectrogram, n_{msh} , T_{msh} , V_{msh} in GSE (Geocentric Solar Ecliptic), V_{msh} relative to \mathbf{B} denoted by sub-indices \parallel and \perp , plasma β_{msh} (red), particle (black), \mathbf{B} -pressure (blue), and $|\mathbf{B}|$.

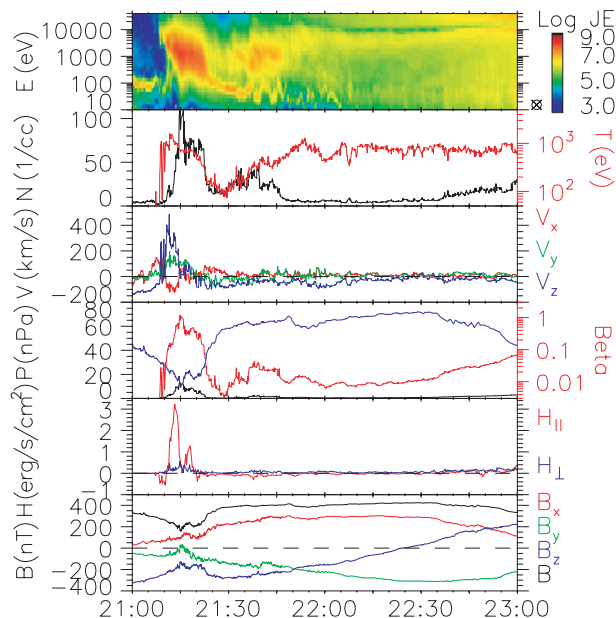


FIG. 3. (Color) Intense ion fluxes are detected by Cluster on the dayside (21 October 2001) at the expected mid-altitude cusp region. SC1 at 2110 UT was at (2.9, -0.23 , -4.57) R_E in GSE ($R_E \sim 6400$ km). Top to bottom, energy flux spectrogram, n and T , V_x , V_y , V_z (GSE), plasma β (red), particle (black) and \mathbf{B} -pressure (blue), heat flux \mathbf{H} and \mathbf{B} field.

The density $n_{msh} \sim 95$ cc $^{-1}$ is about three times the ~ 30 cc $^{-1}$ at L_1 . This increase is attributed to the slowing down of the solar wind and compression across the bow shock. The increase of n_{msh} is common to all of the events studied. We have observed n_{msh} increase up to four times n_{sw} . (We consider only density changes because temperature changes require knowledge about heating mechanisms that are still not clearly understood.)

Note the extremely high β plasma (~ 100 – 1000) in the magnetosheath and V_{\perp} (black) exceeding the local Alfvén speed, $V_A = B_o / (\mu_o n m)^{1/2}$. For this event, V_{\perp} was ~ 200 km s $^{-1}$, $V_A \sim 30$ km s $^{-1}$, and $V_{\perp} > V_A$ for the entire magnetosheath. Inside the magnetosphere, V_{\perp} was ~ 0 km s $^{-1}$ indicating there was no transport across the magnetopause. This behavior is seen for nearly all magnetopause crossings studied, including times when V_{sw} was as low as ~ 300 km s $^{-1}$, when a lower hybrid soliton was detected at the magnetopause¹⁷ and during flux transfer events detected by Cluster¹⁸ (not shown).

C. Mid-Altitude Magnetosphere: Cluster was on the dayside inbound from the southern hemisphere perigee when it encountered an abrupt increase of ion density at ~ 2110 UT flowing along \mathbf{B} with $V_z \sim V_{\parallel} \sim -400$ km s $^{-1}$ lasting until ~ 2116 UT when the density reached a maximum (Fig. 3). The bulk speed was $V_{\perp} \sim 100$ km s $^{-1}$. The ion $T \sim 1$ keV (but anisotropic, $T_{\parallel}/T_{\perp} \sim 3$) and β reached ~ 1 . Note the large heat flux $H_{\parallel} \sim 3$ erg cm $^{-2}$ s $^{-1}$ flowing into the ionosphere. The geomagnetic field underwent large deformation, reducing $|\mathbf{B}|$ from ~ 350 nT ~ 200 nT.

The ~ 110 cc $^{-1}$ peak density measured by SC1 is more than twice the ~ 50 cc $^{-1}$ at L_1 . We do not have direct measurements of n_{msh} by Cluster. However, the transient solar wind compressed the magnetopause and the Geotail space-

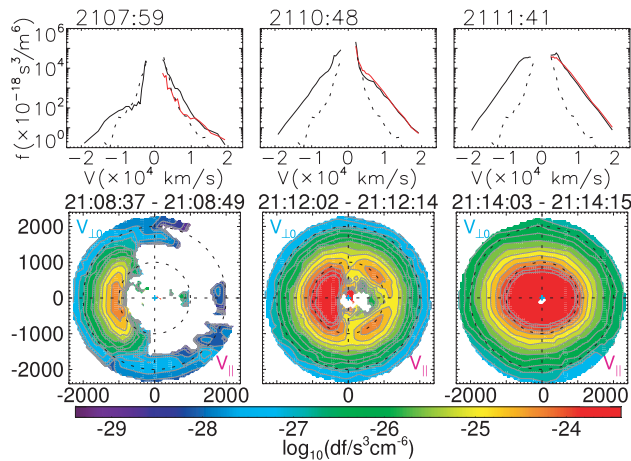


FIG. 4. (Color) Phase-space distributions of electrons (top) and ions (bottom). The electrons are for energies above the spacecraft potential (15 eV). (+) and (-) v_{\parallel} correspond to directions parallel and antiparallel to \mathbf{B} . The “flattop” shape electron distributions are similar to magnetosheath distributions. The ions show mixed magnetosheath, magnetospheric, and ionospheric distributions. Species identifications are made using the ion composition data.

craft crossed into the magnetosheath in the dawn sector (3.4, -20.3 , -0.3) R_E measuring a density of $\sim 30 \text{ cc}^{-1}$ in the energy range 100 eV–45 keV (Not shown). The lower density measured by Geotail is due to a more restricted range of energies measured.

Electron Distributions: The sequence of one-dimensional (1D) cuts of electron phase space distributions (spin average, 4s) parallel (black) and perpendicular (red) to \mathbf{B} show that before entry into the high-density plasma region, the distributions had cold and hot components (Fig. 4). The hot electrons with $-v_{\parallel}$ are electrons coming from the ionosphere. The $-v_{\parallel}$ electrons going toward the ionosphere are initially anisotropic and become nearly isotropic. The distribution turns over at $-v_{\parallel} < 7 \times 10^6 \text{ m s}^{-1}$, forming a “flattop” shape. These flattop shape distributions are similar to shocked solar wind found in the magnetosheath.¹² That such distributions can appear at mid-altitude cusp is consistent with Cluster traversing a region that was connected to the magnetosheath. The temperature of the cold component is $T_e \sim 10\text{--}20 \text{ eV}$ and hot $T_e \sim 60\text{--}100 \text{ eV}$. The current density (\mathbf{J}) deduced from electrons along \mathbf{B} shows a bipolar feature with $J_{\parallel} \sim 400 \text{ nA m}^{-2}$. Heat flux ($H_{\parallel} \sim 0.03 \text{ erg cm}^{-2} \text{ s}^{-1}$) was measured at the leading (trailing) edges flowing into (out of) the ionosphere and in between ($-0.02 \text{ erg cm}^{-2} \text{ s}^{-1}$) was flowing out (not shown).

Ion Distributions: Two-dimensional (v_{\parallel}, v_{\perp}) cuts of 3D ion phase-space distributions (three spin averages) have been computed after subtracting the perpendicular flow from 2107:13–2114:15 UT (Fig. 4). Near the origin of each panel is a low-energy ionospheric beam, which the composition instrument clearly resolves as O^+ (It appears in the spectrogram as the “monoenergetic” 100 eV ions.) The sequence shows a low energy O^+ field aligned beam propagating outward along \mathbf{B} from the ionosphere, a few keV H^+ beam propagating toward the ionosphere, and an isotropic high-energy magnetospheric population. These ions are seen to

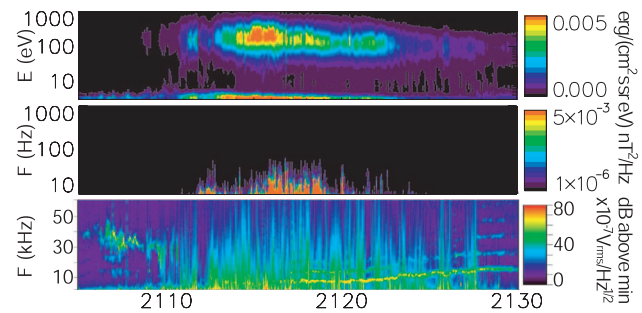


FIG. 5. (Color) A wave spectrogram (21 October 2001). EM waves are electron and ion cyclotron emissions. The broadband ES emissions are produced by deBye-scale electron holes. The narrow emissions at harmonics $\sim (n+1/2)f_{ce}$ are Bernstein mode waves. Density $\sim 22 \text{ cc}^{-1}$ for electrons and protons and $|\mathbf{B}|=240 \text{ nT}$ at 2112 UT yield the following frequencies: cyclotron $f_{ce} \sim 6.73 \text{ kHz}$ and $f_{ci} \sim 3.67 \text{ Hz}$, plasma $f_{pe} \sim 44.3 \text{ kHz}$ and $f_{pi} \sim 972 \text{ Hz}$, lower and upper hybrid $f_{lh} \sim 155 \text{ Hz}$, $f_{uh} \sim 44.8 \text{ kHz}$.

mirror below the spacecraft, and initially exhibit a loss cone for the returning ions. Later, the distributions evolved to a bi-Maxwellian, with $T_{\parallel}(2.5 \times 10^7 \text{ K}) > T_{\perp}(1.5 \times 10^7 \text{ K})$.

Waves: The waves accompanying the mid-altitude cusp particles are electromagnetic (EM) and broadband electrostatic (ES) emissions and electron Bernstein modes at multiples of $\sim (n+1/2)f_{ce}$, where f_{ce} is the electron cyclotron frequency (Fig. 5). The EM emissions are whistler mode waves. The broadband bursty ES waves are due to unresolved solitary electron holes.¹⁹ The broadband ES and Bernstein mode waves are always observed with the transient particles in mid-altitude cusps.

These observations raise many questions about the interaction of the transient solar wind with the magnetosphere. The IMF during the events studied fluctuated considerably and included both northward and southward directions. Our studies indicate solar wind plasma is indeed entering the magnetosphere via the cusps as previously suggested.^{7,11} The nearly equal densities observed at mid-altitude cusps to those in the magnetosheath suggest that the particles may be free streaming along \mathbf{B} . The estimated number of particles entering the cusp for a one-hour transient using a typical $R_E \times R_E$ cusp area⁷ yields $\sim 10^{30}$ particles. This large number is possibly significant. However, observations do not tell us what fraction remains in the magnetosphere or mirrors back to the magnetosheath. Modeling may reveal what fraction of these particles become trapped and contribute to the ring current.

The electron holes could be produced locally by a two-stream instability or come from the high-altitude cusp.²⁰ The Bernstein mode waves are similar to those seen in the plasmasphere and the magnetosphere.¹⁹ They can be excited by a mixture of cold and anisotropic hot electrons with background ions,^{21,22} ion shell distributions,²³ and ion beams propagating perpendicular to \mathbf{B} .²⁴ No models have incorporated ion beams parallel to \mathbf{B} .

Transient particles in the magnetosheath create a considerable amount of disturbance. On 21 October 2001, the transient particles were not only injected into the cusp, but they could have triggered magnetospheric instability (substorm) that produced an intense aurora. Cluster by coincidence de-

tected high fluxes of energetic (>20 keV) O^+ ions precipitating into the ionosphere, while cold ionospheric O^+ ions were flowing out (not shown). This solar wind transient initiated a moderate size magnetic storm.

We need to investigate what processes can transport particles in the cusps nearly unimpeded from the magnetosheath into the magnetosphere. We also need to understand the significance of ionospheric particles that extend out into the magnetosheath and the high β super-Alfvénic bulk flows that accompany solitary waves and FTEs. Some of the cusp events we studied also included tens of keV particles in the transient solar wind. We need to evaluate how these particles are related to the energetic particles observed in high-altitude cusps.^{9,25} Plans are underway to combine data analysis and modeling to enhance our understanding of the physics of solar wind interaction with the magnetosphere.

The research at UC Berkeley is performed under NASA Grant No. NNG04GF23G.

- ¹H. Grad, *Phys. Rev. Lett.* **4**, 222 (1960).
²G. Schmidt, *Phys. Fluids* **5**, 994 (1962).
³S. Ratliff, J. Dawson, and J. Leboeuf, *Phys. Rev. Lett.* **50**, 1990 (1983).
⁴L. Frank, *J. Geophys. Res.* **76**, 5202, DOI: 10.1029/JA076i022p05202 (1971).
⁵W. Heikilla and D. Winningham, *J. Geophys. Res.* **76**, 883 (1971).
⁶P. Escoubet, M. Fehringer, and M. Goldstein, *Ann. Geophys.* **19**, 1197 (2001).
⁷P. Cargill, B. Lavraud, C. J. Owen, B. Grison, M. W. Dunlop, N. Cornilleau-Wehrlin, C.-P. Escoubet, G. Paschmann, T. D. Phan, L. Rezeau, Y. Bogdanova, and K. Nykyri, *Space Sci. Rev.* **118**, 321 (2005).
⁸T. Fritz and J. Chen, *Measurement* **30**, 599 (1999).
⁹J. Chen and T. Fritz, *Surv. Geophys.* **26**, 71 (2005).
¹⁰S. Y. Fu, Q. Zong, Z. Pu, C. Xiao, A. Korth, P. Daly, and H. Reme, *Surv. Geophys.* **26**, 241 (2005).
¹¹B. Lavraud, H. Réme, M. Dunlop, J.-M. Bosqued, I. Dandouras, J.-A. Sauvaud, A. Keiling, T. D. Phan, R. Lundin, P. J. Cargill, C. P. Escoubet, C. W. Carlson, J. P. McFadden, G. K. Parks, E. Moebius, L. M. Kistler, E. Amata, M.-B. Bavassano-Cattaneo, A. Korth, B. Klecker, and A. Balogh, *Surv. Geophys.* **26**, 135 (2005).
¹²W. Feldman, S. Bame, P. Gary, J. Gosling, D. McComas, M. Thomsen, G. Paschmann, N. Sckopke, M. Hoppe, and C. Russell, *Phys. Rev. Lett.* **49**, 199 (1982).
¹³M. Brittnacher, M. Wilber, M. Fillingim, C. Chua, G. Parks, J. Spann, and G. Germany, *Adv. Space Res.* **25**, 1377 (2000).
¹⁴R. Winglee and J. Meneitti, *J. Geophys. Res.* **103**, 9189, DOI: 10.1029/97JA03732 (1998).
¹⁵J. Slavin, C. Owen, M. Dunlop, E. Borälv, M. B. Moldwin, D. G. Sibeck, E. Tanskanen, M. L. Goldstein, A. Fazakerley, A. Balogh, E. Lucek, I. Richter, H. Réme, and J. M. Bosqued, *Geophys. Res. Lett.* **30**, 2208, DOI: 10.1029/2003GL018438 (2003).
¹⁶J. Gosling, *Space Sci. Rev.* **72**, 133 (1995).
¹⁷R. Trines, R. Bingham, M. Dunlop, A. Vaivads, J. Davies, J. Mendoca, L. Silva, and P. Shukla, *Phys. Rev. Lett.* **99**, 205006 (2007).
¹⁸M. Dunlop, B. Lavraud, P. Cargill, M. G. G. T. Taylor, A. Balogh, H. Reme, P. Décreau, K.-H. Glassmeier, R. C. Elphic, J.-M. Bosqued, A. N. Fazakerley, I. Dandouras, C. P. Escoubet, H. Laakso, and A. Marchaudon, *Surv. Geophys.* **26**, 1 (2005).
¹⁹P. Canu, P. Décreau, M. G. G. T. Taylor, A. Vontrat-Reberac, J. G. Trotignon, J. L. Rauch, D. Fontaine, A. Fazakerley, J. Pickett, D. Gurnett, J.-M. Bosqued, N. Cornilleau-Wehrlin, D. Sunkvist, M. Dunlop, and K.-H. Glassmeier (Abstract), *URSI XXVII General Assembly* (2002).
²⁰J. Pickett, J. Franz, J. Scudder, J. Meneitti, D. Gurnett, G. Hospodarsky, R. Braunger, P. Kintner, and W. Kurth, *J. Geophys. Res.* **106**, 19081, DOI: 10.1029/2000JA003012 (2001).
²¹M. Ashour-Abdalla and C. Kennel, *J. Geophys. Res.* **83**, 1531, DOI: 10.1029/JA083iA04p01531 (1978).
²²A. Willes and P. Robinson, *J. Plasma Phys.* **58**, 171 (1997).
²³P. Janhunen, A. Olsson, A. Vaivads, and W. Peterson, *Ann. Geophys.* **21**, 881 (2003).
²⁴A. Brinca, F. Romerías, and L. Gomberoff, *Geophys. Res. Lett.* **30**, 2175, DOI: 10.1029/2003GL017501 (2003).
²⁵S.-W. Chang, J. Scudder, S. Fuselier, J. F. Fennel, K. J. Trattner, J. S. Pickett, H. E. Spence, J. D. Meneitti, W. K. Peterson, R. P. Lepping, and R. Friedel, *Geophys. Res. Lett.* **25**, 3729, DOI: 10.1029/98GL52808 (1998).